Bifurcation analysis of a car and driver model

Fabio Della Rossa[a], Massimiliano Gobbi[b], Gianpiero Mastinu[b*], Carlo Piccardi[a] and Giorgio Previati[b]

[a]*Dipartimento di Elettronica Informazione e Bioingegneria, Politecnico di Milano, Piazza Leonardo da Vinci 32, 20133 Milano, Italy;* [b]*Dipartimento di Meccanica, Politecnico di Milano, Piazza Leonardo da Vinci 32, 20133 Milano, Italy*

(*Received 1 November 2013; accepted 18 January 2014*)

1. Introduction

The dynamic behaviour of a car negotiating a curve or running straight ahead is widely discussed in the literature. In most cases the interest is focused on the vehicle alone (i.e. without driver).[1] However, the vehicle and the driver are two parts of a single system and their interaction can change the overall behaviour of the vehicle. In this paper, the combined dynamic behaviour of the vehicle and the driver is considered. Many different driver models have been presented in the literature, with different applications and scopes.[2] In the following analysis, a preview tracking driver model is considered.[2–8] This model is well suited to describe the lateral vehicle dynamics. The longitudinal dynamics are simply not considered here,[2] even if they are not independent on the steering task of the driver. Actually steering the front wheels causes a component of the lateral tyre force to act along the longitudinal axis of the vehicle. This contribution is usually neglected if the manoeuvre lasts for a very short time. This is the hypothesis under which the two-wheel (or bicycle) model is derived and used. The

*Corresponding author. Email: mastinu@mecc.polimi.it

combination of lateral and longitudinal dynamics can be taken into account as shown in.[1] A discussion about the influence of the driver and the steering system on the dynamic behaviour of a car can be found in.[2,8]

For the majority of situations, actually all those a normal driver is likely to experience, a linear model of the vehicle and a linear model of the tyres are sufficient. There are, however, a number of important situations, mostly related to emergency manoeuvres, in which high slip angles are reached and the nonlinear behaviour of the vehicle plays a crucial role. In such situations, a well-designed vehicle (i.e a vehicle whose nonlinear behaviour has been considered and understood) can make the difference between a tragic accident and a barely notable risky situation.[1,9] Control systems are usually developed and tested on low friction surfaces, so that the nonlinear part of the tyre characteristics is reached. Thus, understanding nonlinear phenomena is of paramount practical importance in order to improve the controls and the active safety of road vehicles.

In this paper, the study of the nonlinear behaviour of a vehicle when negotiating a curve and when running straight ahead is discussed in the framework of bifurcation analysis.[10] This approach allows one to compute and characterise all the possible equilibria of a nonlinear system and has been successfully applied to many aspects of vehicle dynamics and control.[5,11–22] For example, when considering the dynamic behaviour of a road vehicle at high lateral acceleration levels, more than one equilibrium may occur due to the nonlinear characteristics of the tyres.[12,14] In this situation, bifurcation analysis, supported by the handling diagram theory,[23] is a very useful tool for the computation of all the existing equilibria.

The paper is organised as follows. First, the vehicle and driver models are introduced along with a validation against telemetry data of a racing car during a track lap.

Two case studies are discussed, referring either to an understeering (UN) or to an oversteering (OV) vehicle.

The shape and the characteristics of the basins of attraction at different vehicle speeds are presented and discussed.

Finally, a three-parameter bifurcation analysis is performed, referring to driver's gain, driver's prediction time and forward speed.

2. Vehicle and driver models

The mechanical model analysed in this paper is the well-known two degrees of freedom (2 d.o.f.) *single-track model* [1,7,9,23,24] shown in Figure 1.

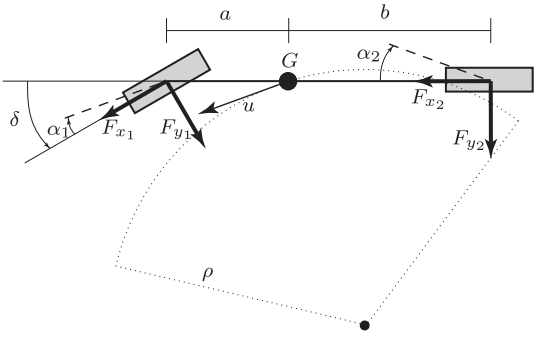

Figure 1. Representation of the single-track model.

The main simplifying hypotheses are:

- the forward speed u is constant;
- the centre of gravity (c.g.) lies at the ground level;
- the vehicle body is modelled referring to its longitudinal axis;
- the resultant of the forces acting at the front and rear axles are applied at the centres of the axles;
- the slip angles α_i, $i = 1, 2$, and the steering angle δ (Figure 1) are small
- no longitudinal forces are acting at the wheels.

2.1. *Vehicle mathematical model*

Under the above hypotheses, the equations of motion read [23]

$$\begin{aligned} m(\dot{v} + ur) &= F_{y_1} + F_{y_2}, \\ I_z \dot{r} &= F_{y_1} a - F_{y_2} b \end{aligned} \tag{1}$$

where u and v are the longitudinal and lateral speeds, respectively, r is the yaw rate, subscripts 1 and 2 refer, respectively, to the front and rear axle, F_{y_i} is the lateral force on the ith axle, m is the vehicle mass, a and b are the distances, respectively, of the front and the rear axle centre from the vehicle's centre of mass, I_z is the moment of inertia of the vehicle around the vertical axis at the c.g. The front and rear slip angles can be obtained through the following equations:

$$\alpha_2 = -\frac{v - rb}{u}, \quad \delta - \alpha_1 = \frac{v + ra}{u}. \tag{2}$$

The lateral forces $F_{y_i}(\alpha_i)$ $(i = 1, 2)$ can be expressed as functions of the slip angles α_i.[23] The functions $F_{y_i}(\alpha_i)$, namely the tyre characteristics, can have very different shapes.[1,23] In this paper, for the sake of space, we will analyse only two different tyre characteristics, which will be presented in Section 2.4.

2.2. *Validation*

The validation of model (1) has been performed considering a sports car. Model simulations have been compared with the telemetry data acquired by the vehicle manufacturer during a lap run. The main parameters of the vehicle are reported in Table 1.

The time history of the steering-wheel angle δ and of the car longitudinal speed u has been considered as the model inputs. The measured yaw rate and lateral acceleration have been compared with the simulated ones. Figure 2 shows a satisfactory agreement between experimental data and simulated outputs.

Despite the very high lateral accelerations attained by the sports car and the simplicity of the model, a reasonable matching of computed and measured data is found because of the

Table 1. Main parameters of a sports car used to validate the vehicle model (1).

	Value	*Unit*
Vehicle mass (m)	550	kg
Vehicle yaw moment of inertia (I_z)	750	kg m^2
Distance from front axle to c.g. (a)	1.64	m
Distance from rear axle to c.g. (b)	0.98	m

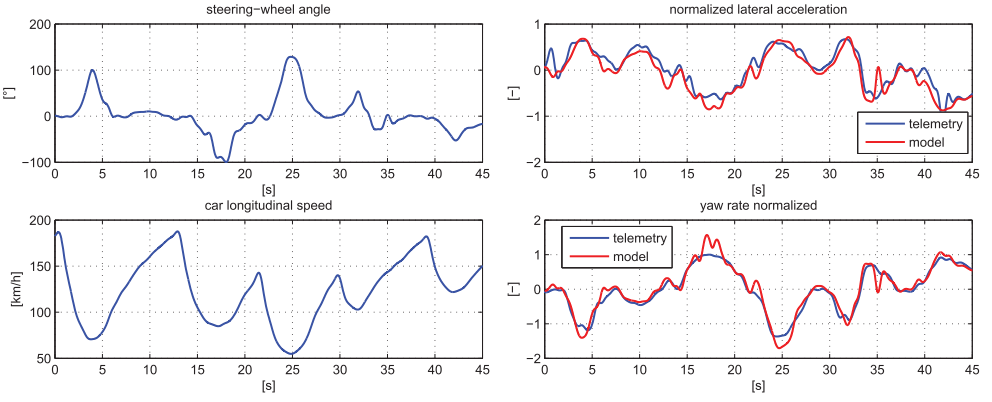

Figure 2. Lateral acceleration and yaw rate (measured and simulated) on a track (right panels). Steering wheel angle and vehicle speed (left panels) are used as model inputs. Vehicle data are reported in Table 1.

stiffness of the suspension system that makes the tyres considerably influence the dynamic behaviour of the car.

It must be acknowledged that this validation study only confirms that model (1), namely a 2 dof model with nonlinear lateral tyre forces, is capable of good agreement with measured responses, at least in this case study (we anticipate that the bifurcation analyses of Sections 4–6 will be carried out with different parameter values). Although this does not ensure that the model is able to accurately describe the stability properties of any generic car, since much more extensive and detailed tests would be required, it is nonetheless a fact supporting the validity of model (1).

2.3. *Driver model*

We adopt the driver model described in [2,3,7] and based on the block diagram of Figure 3.

The driver chooses a desired trajectory y_{nom} referring to a specified curvature, and so the steering angle is set at a certain value δ_{nom}. While steering, the current position y is compared with the desired one, the error being Δy. Then the error Δy_{P} in a nearby future time $t + T_{\text{P}}$ is predicted by a prediction block $G_{\text{P}}(s)$. Based on this prediction, the steer angle $\Delta\delta$ is applied, through the control block $G_{\text{C}}(s)$. A new steer angle δ is so applied, which is the input to the vehicle model (1) which gives as a result the new position y on the trajectory.

The following assumptions are made on the way the driver predicts and compensates the error Δy. For the prediction, we simply assume that the driver can exactly anticipate the error Δy by a certain time T_P, so that the transfer function $G_{\text{P}}(s)$ will be simply $e^{T_P s}$. For the control, we assume that the driver has a certain delay τ to react, and then she/he gets convergence with a time constant T_{C}. So $G_{\text{C}}(s)$ is the first-order transfer function $e^{-\tau s} k_{\text{C}}/(1 + T_{\text{C}} s)$, where k_{C} is the gain of the transfer function. The complete transfer function from the error Δy to the

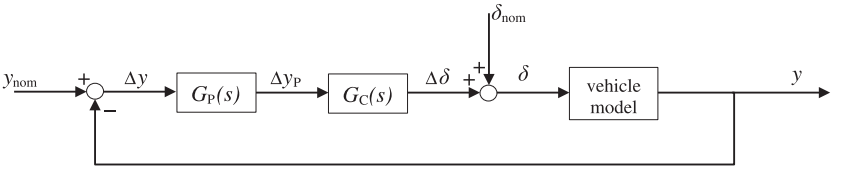

Figure 3. Block diagram of the driver model.

control signal $\Delta\delta$ is

$$\Delta\delta = \mathrm{e}^{T_{\mathrm{P}}s}\mathrm{e}^{-\tau s}k_{\mathrm{C}}\frac{1}{1+T_{\mathrm{C}}s}, \quad \Delta y = \mathrm{e}^{(T_{\mathrm{P}}-\tau)s}k_{\mathrm{C}}\frac{1}{1+T_{\mathrm{C}}s},$$
$$\Delta y \cong k_{\mathrm{C}}\frac{1+(T_{\mathrm{P}}-\tau)s+(1/2)((T_{\mathrm{P}}-\tau)s)^2}{1+T_{\mathrm{C}}s}\Delta y,$$

where the exponential function has been approximated by a truncated Taylor series, as in [7]. Notice that this approximation is valid only for low-frequency corrections (approximately less than 0.2 Hz).

Let us describe how δ_{nom} can be computed, i.e. how the desired trajectory y_{nom} (referring to a given curvature $1/\rho$, where ρ is the radius of the bend) can be attained. Notice that specifying δ_{nom} means that the system vehicle+driver will run into the bend at a certain steady-state couple of lateral and angular speed $(v_{\mathrm{R}}, r_{\mathrm{R}})$. Such a couple satisfies Equation (1), i.e. it satisfies the steady-state equilibrium of the bare vehicle running into a bend with $\delta = \delta_{\mathrm{nom}}$. The longitudinal speed u is kept constant by hypothesis, and only the lateral displacement from the trajectory Δy is used for control. Under this assumption, the error in position (both lateral displacement Δy and angular displacement ϑ) is simply given by

$$\Delta\dot{y} = v_{\mathrm{R}}\cos\vartheta - u\sin\vartheta - v,$$
$$\dot{\vartheta} = r - r_{\mathrm{R}}.$$

Summarising, the complete mathematical model for the vehicle+driver is

$$\begin{aligned} m(\dot{v}+ur) &= F_{y_1}(v,r,\delta_{\mathrm{nom}}+\Delta\delta) + F_{y_2}(v,r),\\ I_z\dot{r} &= F_{y_1}(v,r,\delta_{\mathrm{nom}}+\Delta\delta)a - F_{y_2}(v,r)b,\\ T_{\mathrm{C}}\Delta\dot{\delta} &= k_{\mathrm{C}}(\Delta y + (T_{\mathrm{P}}-\tau)\Delta\dot{y} + 1/2(T_{\mathrm{P}}-\tau)^2\Delta\ddot{y}) - \Delta\delta,\\ \Delta\dot{y} &= v_{\mathrm{R}}\cos\vartheta - u\sin\vartheta - v,\\ \dot{\vartheta} &= r - r_{\mathrm{R}}, \end{aligned} \tag{3}$$

where

$$\Delta\ddot{y} = -v_{\mathrm{R}}\sin\vartheta\dot{\vartheta} - u\cos\vartheta\dot{\vartheta} - \dot{v}.$$

Notice that the complete model is a fifth-order model in which the state variables are v, r, $\Delta\delta$, Δy, ϑ. The only equilibria that will be considered for this model are of the type

$$\begin{aligned} v &= v_{\mathrm{R}},\\ r &= r_{\mathrm{R}},\\ \Delta\delta &= 0,\\ \Delta y &= 0,\\ \vartheta &= 0, \end{aligned} \tag{4}$$

as explained and discussed in Section 3. Notice that, by means of Equation (2), the state variables (v, r) can be interchanged with (α_1, α_2).

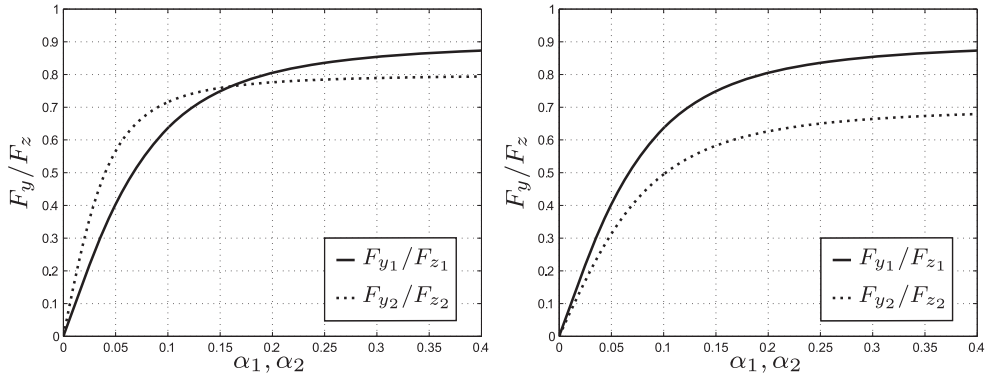

Figure 4. Tyre characteristics. The left panel refers to an understeering vehicle at low centripetal acceleration (UN case). The right panel refers to an OV case.

Table 2. The parameter set of model (3)–(5).

Vehicle		*Driver*		*Front tyre*			*Rear tyre*		
					UN	OV		UN	OV
Mass m	950 kg	Control time T_C	0.2 s						
Principal inertia moment I_z	1100 kg m^2	Control delay τ	0.2 s	B_1	10	10	B_2	20	10
Wheelbase l	2.46 m	Prediction time T_P	0.7 s	C_1	1	1	C_2	1	1
a	0.95 m	Control gain k_C	$\frac{k_{MAX} - 0.3u}{u} \frac{\text{rad}}{\text{m}}$	E_1	0	0	E_2	0	0
b	1.51 m	Maximum control gain k_{MAX}	$50 \frac{\text{rad}}{\text{m}}$	μ_1	0.9	0.9	μ_2	0.8	0.7

Notes: Vehicle and wheel parameters are taken from [1], while driver parameters are taken from [7] (k_C as a function of the forward speed u is obtained fitting the values reported in [7], Figure 120.7).

2.4. *Case studies*

With respect to the analysis performed in,[1] we consider here two cases only. In the first case a vehicle is fitted with tyres whose characteristics are depicted on the left panel of Figure 4. Such a vehicle has an understeering behaviour at low lateral acceleration (UN case). In the second case the same vehicle is fitted with tyres whose characteristics are depicted in the right panel of Figure 4. The vehicle has an oversteering behaviour at any lateral acceleration (OV case).

The tyre characteristics are defined through the formulae proposed in,[11] which read

$$\begin{aligned} F_{y_1}(\alpha_1) &= D_1 \sin(C_1 \tan^{-1}(B_1\alpha_1 - E_1(B_1\alpha_1 - \tan^{-1}(B_1\alpha_1)))), \quad F_{z_1} = \mu_1 mg\frac{b}{l}, \\ F_{y_2}(\alpha_2) &= D_2 \sin(C_2 \tan^{-1}(B_2\alpha_2 - E_2(B_2\alpha_2 - \tan^{-1}(B_2\alpha_2)))), \quad F_{z_2} = \mu_2 mg\frac{a}{l}, \end{aligned} \tag{5}$$

where

$$D_1 = \mu_1 \frac{mg}{l} b, \quad D_2 = \mu_2 \frac{mg}{l} a,$$

with parameters reported in Table 2.

3. Computation of equilibria

For bifurcation analysis it is imperative to rely on a computational method that provides all the existing equilibria of the system. In [1,23] the powerful *handling diagram* method is exploited with this aim. For the vehicle running into a bend at a fixed steering angle δ, the motion is described by the second-order dynamical system (1), while the mathematical model of the system composed of vehicle and driver is the fifth-order dynamical system (3). We investigate whether the handling diagram method, used in [1,23] for the second-order system (1), can be exploited to compute the equilibria of the vehicle+driver system. The answer we illustrate here is positive, under the hypotheses that the vehicle+driver system runs into a bend at a constant forward speed u and that we look exclusively at the steady-state equilibria defined by Equation (4). Such equilibria are defined by $\Delta\delta = 0$, $\Delta y = 0$, $\vartheta = 0$, and additionally we set $v = v_R$ and $r = r_R$ in such a way that the steady-state lateral slips α_1, α_2 of the vehicle with driver are equal to the corresponding steady-state lateral slips (α_1, α_2) for the vehicle without driver (notice that, by means of Equation (2), the state variables (v, r) can be interchanged with the state variables (α_1, α_2)). Such hypotheses are quite general and do not limit the cases that can be studied both theoretically and in practice.

4. Vehicle without driver control

4.1. *Understeering vehicle without driver*

Let us consider a vehicle defined by Equation (1) and whose parameters are those in Table 2 (case UN). The vehicle runs at a constant steer angle $\delta = 0.05$ rad $\approx 2.86°$ at different constant forward speeds u.

In the phase portrait of Figure 5(a) three steady states are present (depicted in Figure 6):

- In e_2 the vehicle is turning leftward, making an anti-clockwise circle of radius $\rho = l/(\delta + \alpha_2 - \alpha_1)$ approx 60 m: this equilibrium is stable, i.e. the vehicle steadily runs along this trajectory. All the perturbations that move the slip angles in the grey region (basin of attraction) are naturally reabsorbed from the system.
- In e_1 the vehicle is turning leftward, making an anti-clockwise circle of radius $\rho \sim 13$ m : this equilibrium is a saddle, i.e. a perturbation from the equilibrium may not naturally be reabsorbed from the system which may diverge, or converge to the equilibrium e_2.

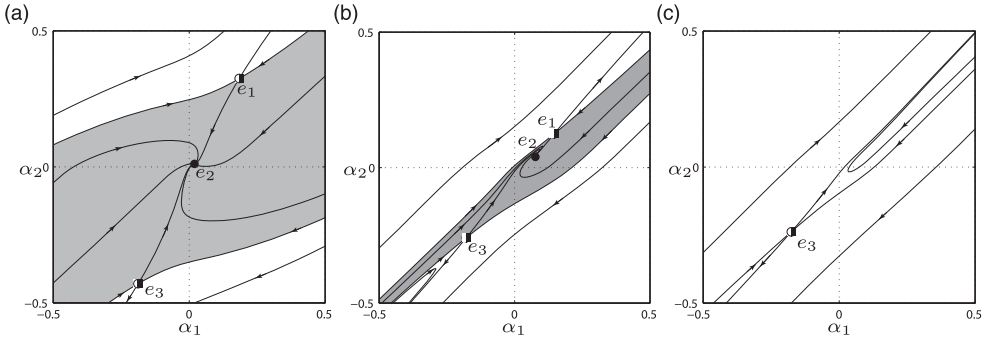

Figure 5. Vehicle without driver. Phase portraits of Equation (1) (case UN) at different speeds, steer angle $\delta = 0.05$ rad. (a) $u = 10$ m/s. (b) $u = 20$ m/s. (c) $u = 40$ m/s.

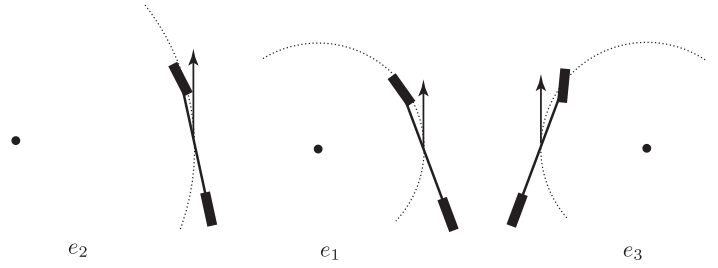

Figure 6. Steady-state attitudes of the vehicle of Figure 5(a) at the three possible equilibria e_2, e_1, and e_3.

- In e_3 the vehicle is turning rightward, making a clockwise circle of radius $\rho \sim 13$ m while counter steering: also in this case the equilibrium is a saddle.

In the phase portrait of Figure 5(b) three possible steady states are also present: e_2 and e_1, in which the vehicle is turning leftward (respectively on circles of radius 90 and 50 m), and e_3, in which the vehicle is turning rightward (on a circle of radius 50 m).

In the phase portrait of Figure 5(c) a critical forward speed at which equilibria e_2 and e_1 collide and disappear into a *saddle-node bifurcation* (this takes place at $u \approx 35$ m/s) has been exceeded. The vehicle at this forward speed and with this steering angle cannot turn leftward, but only rightward (on a circle of radius 200 m), on the saddle equilibrium e_3. No stable steady-state behaviour exists.

4.2. *Oversteering vehicle without driver*

Let us now consider a vehicle defined by Equation (1) and whose parameters are those in Table 2 (case OV). The vehicle runs at a constant steer angle $\delta = 0$ rad at different constant forward speeds u.

In Figure 7(a) the phase portrait shows that three possible steady states are present: e_2, at which the vehicle does not turn, i.e. it runs straight ahead, e_1 in which the vehicle is turning leftward, and e_3, in which the vehicle is turning rightward (on circles of radius 90 m).

In Figure 7(b) the only steady state present is e_2, in which the vehicle does not turn: in this case, however, the vehicle is unstable (the equilibrium is a saddle). In fact, we are again above a critical forward speed ($u \approx 27.6$ m/s) in which e_1 and e_3 collide with e_2 and then disappear into a *pitchfork bifurcation*.

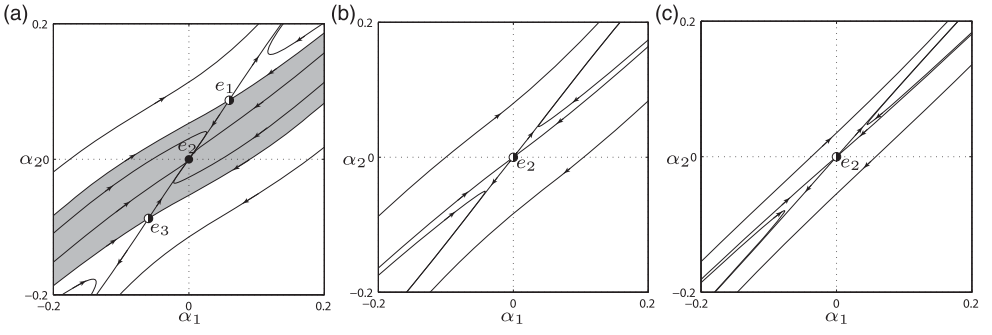

Figure 7. Vehicle without driver. Phase portraits of Equation (1) (case OV) at different speeds, steer angle $\delta = 0.0$ rad. (a) $u = 20$ m/s. (b) $u = 30$ m/s. (c) $u = 60$ m/s.

Figure 6(c) is qualitatively equivalent to Figure 6(b). Bifurcation analysis and continuation techniques [10,25,26] allow us to state that equilibrium e_2 will remain a saddle also for larger longitudinal speed.

5. Vehicle with driver control

Let us consider the vehicle+driver system defined by Equations (3) and whose parameters are those in Table 2. Following the discussion in Section 3 we can state that, at steady state, the values of the lateral slips (α_1, α_2) of the vehicle+driver system are the same of the vehicle without driver. This occurrence, representing quite fairly the actual behaviour of a vehicle running into a bend, is obtained by setting $v_R = ((\delta - \alpha_1)b - a\alpha_2)u/l, r_R = (\alpha_2 - \alpha_1 + \delta)u/l$ at each equilibrium where (α_1, α_2) are the lateral slips computed by the handling diagram theory [1] for the bare vehicle defined by Equation (1). Therefore at each equilibrium of the vehicle+driver system, we have $v = ((\delta_{nom} - \alpha_1)b - a\alpha_2)u/l$, $r = (\alpha_2 - \alpha_1 + \delta_{nom})u/l$, $\Delta y = 0$, $\vartheta = 0$, $\Delta\delta = 0$.

The analysis of the equilibria of a vehicle cornering into a bend has been already presented in the previous section. Such equilibria are the same for the vehicle+driver. Obviously, the nature of the equilibria can change due to the action of the driver that can make stable an unstable equilibrium and vice versa.

We will analyse a limited but relevant number of cases by performing a preliminary bifurcation analysis by varying a single parameter, namely the forward speed u. We will consider the steady states discussed in Section 4 and we will derive the phase portrait of the vehicle+driver system projected on the state variables plane (α_1, α_2).

In order to compare the stability properties of the equilibrium, also a sort of basin of attraction, restricted to initial condition with only slip angles not at equilibrium values, will be computed. In fact, projecting the five-dimensional basin of attraction on the (α_1, α_2)-plane could be misleading [27]: we thus decided not to show the projection, but the section of the basin of attraction on the plane $\Delta y = \vartheta = \Delta\delta = 0$.

5.1. *Understeering vehicle with driver*

The three panels of Figure 8 describe the behaviour, with driver, around the equilibria e_2, e_1, and e_3 of Figure 5(a). More precisely the equilibrium e_2 in Figure 8(a) coincides with the one in Figure 5(a): one may notice that the grey area is larger, i.e. the basin of attraction is

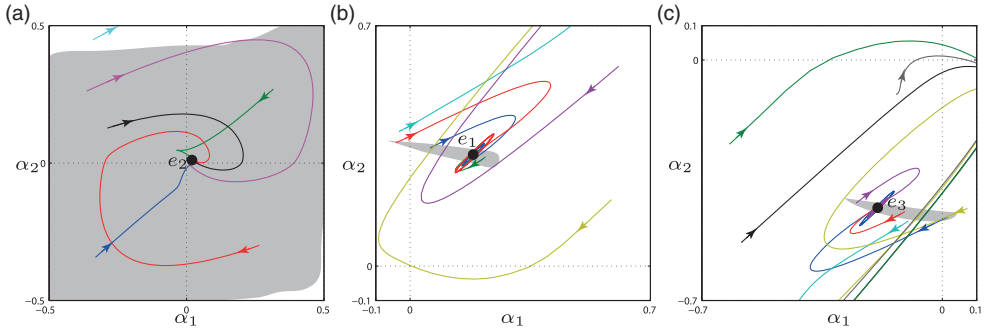

Figure 8. Vehicle with driver. Phase portraits of Equation (3) (case UN) at speed $u = 10$ m/s, steer angle $\delta_{nom} = 0.05$ rad. Projection of the trajectories on the plane (α_1, α_2). Equilibria e_2, e_1, and e_3 correspond to the equilibria e_2, e_1, and e_3 of Figure 5(a).

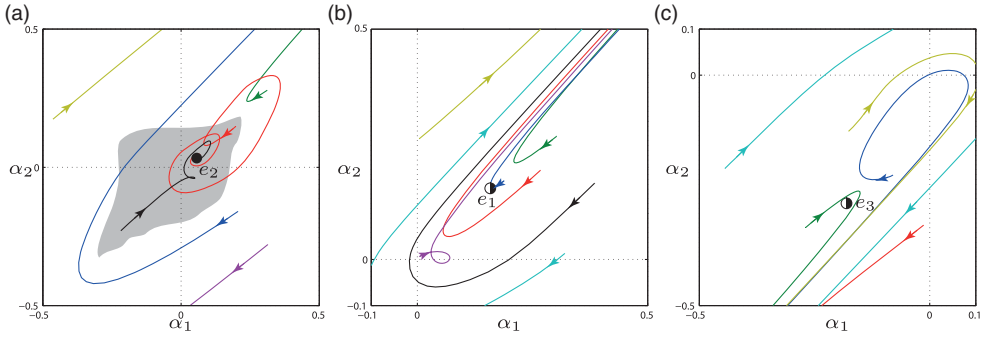

Figure 9. Vehicle with driver. Phase portraits of Equation (3) (case UN) at speed $u = 20\,\mathrm{m/s}$, steer angle $\delta_{\mathrm{nom}} = 0.05\,\mathrm{rad}$. Projection of the trajectories on the plane (α_1, α_2). Equilibria e_2, e_1, and e_3 correspond to the equilibria e_2, e_1, and e_3 of Figure 5(b).

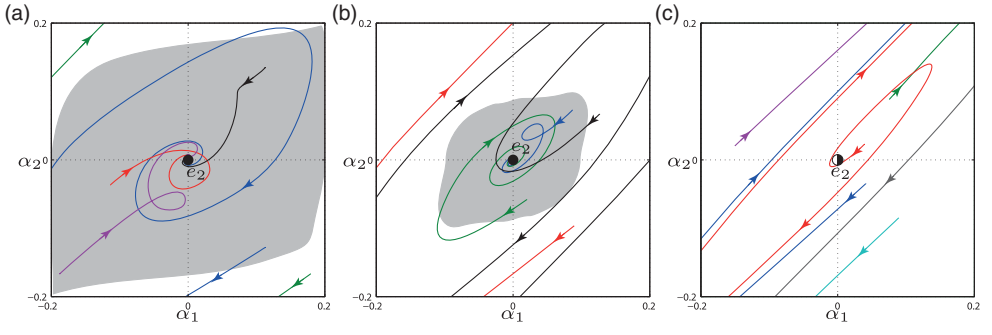

Figure 10. Vehicle with driver, running straight ahead. Phase portraits of Equation (3) (case OV) at different speeds, steer angle $\delta_{\mathrm{nom}} = 0.0\,\mathrm{rad}$. (a) $u = 20\,\mathrm{m/s}$. (b) $u = 30\,\mathrm{m/s}$. (c) $u = 60\,\mathrm{m/s}$. Projection of the trajectories on the plane (α_1, α_2).

broadened. The driver has a stabilising effect. For the equilibrium e_1 (Figure 8(b)), one may notice that the driver has a stabilising effect even in a tight curve (without driver's control the bare vehicle would be unstable). Finally, for the equilibrium e_3 (Figure 8(c)), one may notice that the driver has a stabilising effect even in a counter steering manoeuvre. Notice that we have chosen here a relatively skilled driver and that, although stable, the equilibria e_1 and e_3 have a rather small basin of attraction.

The panels in Figure 9 refer to the case of Figure 5(b) (larger forward speed). Again, for the equilibrium e_2 (Figure 9(a)), one may notice that the grey area is larger, i.e. the basin of attraction is broadened. The driver has a stabilising effect. For the equilibrium e_1 and e_3 instead (Figure 9(b) and 9(c)), one may notice that the driver does not manage to stabilise the already unstable vehicle.

5.2. *Oversteering vehicle with driver*

The phase portraits in Figure 10, referring to the vehicle+driver system, have been obtained starting from the ones in Figure 7 (vehicle without driver). The lateral slips (α_1, α_2) at steady state corresponding to equilibria e_2 are the same for both the vehicle+driver case (Figure 10) and the vehicle without driver (Figure 7).

Let us analyse Figure 10(a): one may notice that the grey area is larger, i.e. the basin of attraction is broadened. The driver has a stabilising effect. Also in Figure 10(b) one may notice that the driver has a stabilising effect (without driver's control the bare vehicle would

be unstable). On the contrary, in the case of Figure 10(c) the driver does not manage to stabilise the vehicle.

6. Bifurcation analysis of a vehicle+driver model running straight ahead at different speeds

In this section, we investigate in detail a simple but important case, namely the motion straight ahead, and we perform a bifurcation analysis of the vehicle+driver model with respect to the speed u and to two of the parameters characterising the driver (Table 2), namely the control gain k_C and the predictive capability of the response of the vehicle, described by the preview time T_P-τ (the greater the preview time, the greater the predictive capability of the response of the vehicle). We compare the results with the behaviour of the vehicle alone.

6.1. *Understeering vehicle*

In the previous section, we already discussed the behaviour of the system in a simplified form, namely for a few fixed values of the speed. Bifurcation analysis allows to portrait the vehicle behaviour when the speed is increased continuously. For the understeering vehicle running straight ahead at speed u, we obtain the bifurcation diagrams of Figure 11: α_1 and α_2 are the front and rear lateral slips, respectively.

At straight running, the steady-state lateral slips are obviously $\alpha_1 = \alpha_2 = 0$. The left panel of Figure 11 points out that, without driver, there are two additional (unstable) equilibria with $\alpha_1 \neq 0, \alpha_2 \neq 0$, i.e. the car is running into bends even with $\delta = 0$ rad (equilibria e_1 and e_3 of Figure 5a). Such additional equilibria define the border of the basin of attraction of $\alpha_1 = \alpha_2 = 0$ (Figure 5): no local bifurcations take place (actually there are global bifurcations, as reported in [1]). At low speed, the stable equilibrium $\alpha_1 = \alpha_2 = 0$ is a node, and it becomes a focus for $u > 15$ m/s. The basin of attraction shrinks until about $u = 40$ m/s, then it remains almost unchanged. Thus, the vehicle without driver is stable up to very high speeds, although the motion is underdamped, i.e. convergence to the equilibrium takes place with damped oscillations.

In the right panel of Figure 11, the vehicle+driver model is considered. We see that the two additional equilibria with $\alpha_1 \neq 0$, $\alpha_2 \neq 0$ no longer exist. Actually, the driver controls

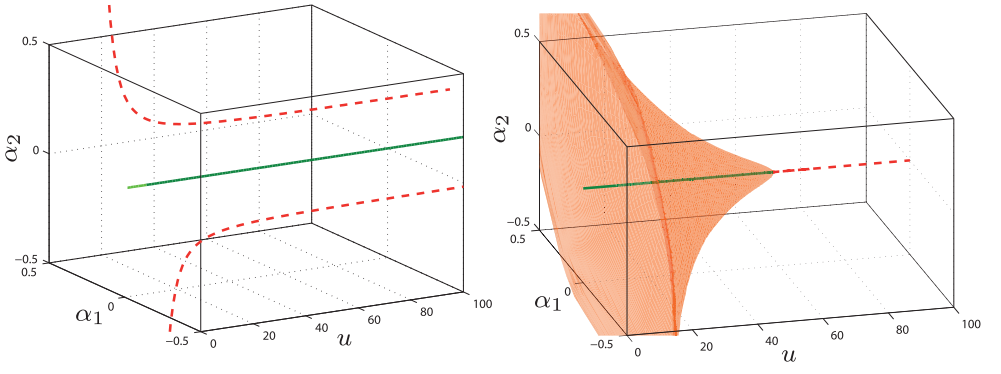

Figure 11. Bifurcation analysis of an understeering vehicle running at forward speed u. Left panel: vehicle without driver (Equation (1), fixed steer, $\delta = 0$). Right panel: vehicle with driver (Equation (3), running straight ahead, $\delta_{nom} = v_R = r_R = 0$). Solid lines are stable equilibria (light if nodes, dark if foci) while dashed lines are unstable equilibria. The surface in the right panel is a family of unstable limit cycles.

the motion along a straight line, and running into bend is not allowed. At low speed, the driver makes the only equilibrium $\alpha_1 = \alpha_2 = 0$ a focus (the bare vehicle has a node). Notably, the driver is unable to run straight ahead at (very) high speed. Indeed, an unstable equilibrium branch initiates at about $u = 60\,\mathrm{m/s}$, where a subcritical Hopf bifurcation is found. Even before, a sufficiently strong disturbance makes the vehicle+driver quite uncontrollable, because the basin of attraction of $\alpha_1 = \alpha_2 = 0$ shrinks approaching the Hopf point. This occurrence is extremely important for understanding what happens in actual cases after a wind gust or an even mild collision. These findings might shed light on a number of apparently odd road accidents.

6.2. *Oversteering vehicle*

In Figure 12, the bifurcation analysis in the oversteering case is reported. At straight running, the steady-state lateral slips are $\alpha_1 = \alpha_2 = 0$. As noted before (Figure 7), the vehicle without driver has two additional equilibria with $\alpha_1 \neq 0, \alpha_2 \neq 0$. They both collide with $\alpha_1 = \alpha_2 = 0$ in a subcritical pitchfork bifurcation at $u = 27.6\,\mathrm{m/s}$. Up to this bifurcation, the stable equilibrium $\alpha_1 = \alpha_2 = 0$ is a node, and its basin of attraction shrinks continuously and eventually disappears at the bifurcation.

In the right panel of Figure 12, the vehicle+driver model is considered. The two additional equilibria with $\alpha_1 \neq 0$, $\alpha_2 \neq 0$ no longer exist, as discussed in the previous section. Due to the driver control, the low-speed equilibrium becomes a focus (the bare vehicle only has a node). Notably, the driver is able to stabilise the vehicle up to larger values of the speed ($u = 41.1\,\mathrm{m/s}$), until a subcritical Hopf bifurcation takes place. As in the previous case, a sufficiently strong disturbance makes the vehicle+driver system quite uncontrollable.

6.3. *Analyzing the role of driver's parameters*

The performance of the driver is mainly influenced by two parameters, namely the gain k_C and the immediacy of the response ($T_P - \tau$). By means of bifurcation analysis, we want to investigate how the stability border (which corresponds to the subcritical Hopf bifurcation, see above) is influenced by these two parameters. The results are summarised in Figure 13: the bifurcation curves have been obtained by standard continuation procedures [10,25,26] using

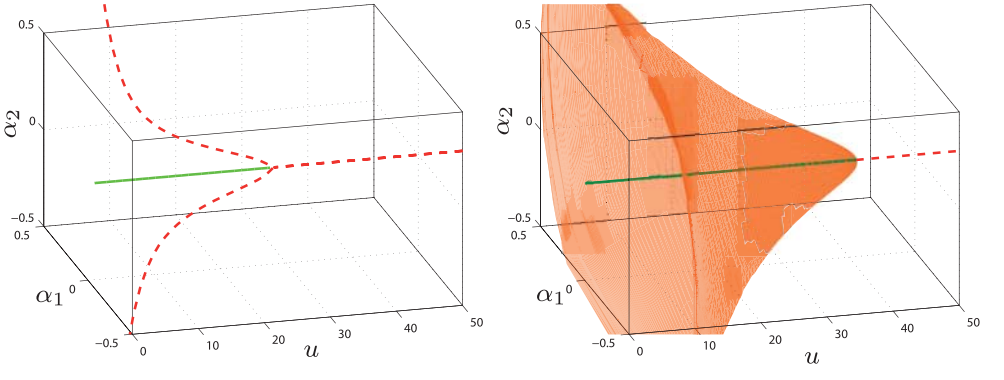

Figure 12. Bifurcation analysis of an OV running at forward speed u. Left panel: vehicle without driver (Equation (1), fixed steer, $\delta = 0$). Right panel: vehicle with driver (Equation (3), running straight ahead, $\delta_{\mathrm{nom}} = v_R = r_R = 0$). Solid lines are stable equilibria (light if nodes, dark if foci) while dashed lines are unstable equilibria. The surface is an unstable limit cycle.

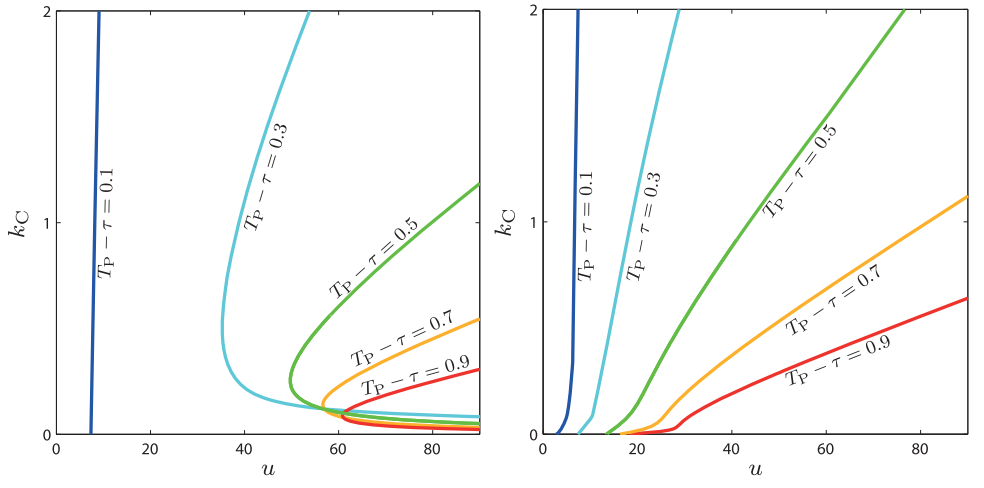

Figure 13. Bifurcation analysis of the oversteering (left) and of the understeering (right) vehicle+driver with respect to the forward speed u and to the driver's gain k_C, for different prediction times of vehicle response ($T_P - \tau$), (the larger the prediction time $T_P - \tau$, the better the prediction of vehicle response). For parameter values in the leftmost side of the plane (small u), the straight motion is asymptotically stable. By varying the parameter values, when crossing a curve from left to right the equilibrium becomes unstable through subcritical Hopf bifurcation. Data in Table 2 and Figure 4.

k_{MAX}, u and $(T_P - \tau)$ as free parameters. For the sake of clarity, in the figure the results are displayed as functions of k_C, which is related to k_{MAX} as specified in Table 2.

The two panels of Figure 13, referring to the oversteering and to the understeering vehicle respectively, show analogies but also important differences. In both cases, and for all $(T_P - \tau)$, the straight ahead motion of the vehicle+driver is stable if u is sufficiently small (i.e. for parameters close to the vertical axis). Moving the parameters rightward in the (u, k_C) plane, the stability is lost (via subcritical Hopf bifurcation) when the relevant curve is crossed. But, as testified by Figures 11 and 12, the control of the vehicle becomes more and more problematic even before the bifurcation takes place, since the basin of attraction progressively shrinks until it annihilates at the bifurcation point.

For the OV (left panel), the positive slope of the curves implies that a more reactive driver (larger gain) is able to keep the system stable up to larger speed values u. This result, somehow counterintuitive, is a consequence of the idealisation of the driver, who is actually equipped with a perfect predictor. Consistently, the stability range increases not only with k_c but also with $(T_P - \tau)$. Indeed, the more effective the predictive capabilities are (i.e. larger $(T_P - \tau)$), the more extended can be the range of stable speeds manageable by a reactive driver (i.e. large gain values k_C). This confirms that the ideal skills of the driver of an OV are a blend of good predicting capability and strong reaction to trajectory mismatching.

For the understeering vehicle (right panel) we first notice that, for a driver with very limited predictive capabilities (i.e. small $(T_P - \tau)$), the behaviour is analogous to the oversteering case (compare the curves with $(T_P - \tau) = 0.1$). The main difference, however, is that now a driver with very small reactivity (small k_C) may completely avoid the loss of stability: this is a consequence of the fact that, contrary to the oversteering case, the uncontrolled vehicle is stable even at large speeds (Figure 11). For medium–large k_C values, on the other hand, the bifurcation portrait is qualitatively the same as in the oversteering case, although there are quantitative differences that could be usefully exploited at design stage.

Overall, comparing the two diagrams, it turns out that an OV vehicle is more challenging to be controlled, *ceteris paribus*, than an understeering one. As a matter of fact, given a driver

identified by the pair (k_C, ($T_P - \tau$)), the range of speeds u that she/he is able to stabilise is systematically smaller in the oversteering case.

7. Conclusions

In the first section of the paper, a nonlinear vehicle+driver model has been developed. The model has been taken from the literature, and fairly represents the state-of-the art knowledge available to date on vehicle–driver interaction. The vehicle model is the well-known 2 d.o.f. model. The driver model is one of the simplest but still more effective presently available. The vehicle model has been validated, showing that, at least for a racing car with very stiff suspensions, the considered vehicle model, although very simple, is able to correctly predict the behaviour of the vehicle at high acceleration levels and at high speeds.

Two case studies are addressed in the paper, referring either to an understeering or to an oversteering vehicle. In Sections 4 and 5, a preliminary bifurcation analysis of the vehicle+driver model has been carried out. The first result is that equilibria of the vehicle+driver model are strictly related to the ones of the vehicle without driver. More precisely, the steady-state lateral slips (α_1, α_2) of the vehicle+driver model are equal to the corresponding steady-state lateral slips (α_1, α_2) of the vehicle without driver. This occurrence allows one to exploit the analysis of equilibria already presented in a previous paper.[1] In the cases that have been proposed and analysed, the driver is able to widen the basin of attraction and, in some cases, to make stable the unstable equilibria pertaining to the bare vehicle. In some cases, however, the driver is not able to stabilise the vehicle.

In Section 6 of the paper, a complete bifurcation analysis has been performed referring to straight ahead motion. At first a bifurcation analysis has been performed by varying the forward speed of the vehicle. It appears that for the vehicle+driver model both the UN and the OV cases have a limit forward speed at which a subcritical Hopf bifurcation occurs. The bare understeering vehicle (without driver) would not have such a limit speed, so it is the driver who introduces a negative effect. On the other hand, a skilled driver is able to make stable an OV vehicle and run at a faster speed than an uncontrolled vehicle.

Then a three-parameter bifurcation analysis is performed, referring to driver's gain, driver's prediction time and vehicle forward speed. The OV is more challenging to be controlled than the UN one.

The results of the paper fully agree with practice. Actually it is well known that the driver may make unstable a vehicle that is inherently stable. Also, it is well known from practice that a skilled driver may make stable an unstable vehicle. The novelty of the paper is having formalised such conjectures and having proved the existence, at least for straight ahead motion, of a subcritical Hopf bifurcation. Being aware of such a bifurcation can help the designers of vehicle controls in enhancing active safety.

References

[1] Della Rossa F, Mastinu G, Piccardi C. Bifurcation analysis on an automobile model negotiating a curve. Vehicle Syst Dyn. 2012;50:1539–1562.
[2] Plöchl M, Edelmann J. Driver models in automobile dynamics application. Vehicle Syst Dyn. 2007;45:699–741.
[3] Apel A, Mitschke M. Adjusting vehicle characteristics by means of driver models. Int J Vehicle Des. 1997;18: 583–596.
[4] Hoffmann ER. Human control of road vehicles. Vehicle Syst Dyn. 1976;5:105–126.
[5] Hu HY, Wu ZQ. Stability and hopf bifurcation of four-wheel-steering vehicles involving driver's delay. Nonlinear Dyn. 2000;22:361–374.
[6] MacAdam CC. Understanding and modeling the human driver. Vehicle Syst Dyn. 2003;40(1–3):101–134.

[7] Mitschke M, Wallentowitz H. Dynamik der Kraftfahrzeuge (4th ed. – in German). Berlin: Springer; 2004.
[8] Gobbi M, Mastinu G, Previati G, De Filippi R, Lunetta I, Moscatelli D. Optimal design of an electric power steering system for sport cars. 23rd international symposium on dinamics of vehicles on roads and tracks; 2013, August 19–23; Qingdao, China.
[9] Mastinu G, Della Rossa F, Piccardi C. Nonlinear dynamics of a road vehicle running into a curve. Applications of chaos and nonlinear dynamics in science and engineering. Vol. 2, Berlin: Springer; 2012. p. 125–153.
[10] Kuznetsov Yu A. Elements of applied bifurcation theory. 3rd ed. New York: Springer; 2004.
[11] Andrzejewski R, Awrejcewicz J. Nonlinear dynamics of a wheeled vehicle. Berlin: Springer; 2005.
[12] Bruni S, Mastinu G. (eds.). Proceedings of the 19th IAVSD symposium: dynamics of vehicles on roads and tracks; 2005; Milan, Italy.
[13] Catino B, Santini S, Di Bernardo M. MCS adaptive control of vehicle dynamics: an application of bifurcation techniques to control system design. Proceedings of the 42nd IEEE conference on decision and control; 2003; Maui, Hawaii. p. 2252–2257.
[14] Hedrick K. (ed.), Proceedings of the 20th IAVSD symposium: dynamics of vehicles on roads and tracks. Berkeley, CA, USA; 2007.
[15] Liaw D-C, Chung W-C. A feedback linearization design for the control of vehicle's lateral dynamics. Nonlinear Dyn. 2008;52(4):313–329.
[16] Liu Z, Payre G, Bourassa P. Nonlinear oscillations and chaotic motions in a road vehicle system with driver steering control. Nonlinear Dyn. 1996;9:281–304.
[17] Ono E, Hosoe S, Tuan HD, Doi S. Bifurcation in vehicle dynamics and robust front wheel steering control. IEEE Trans Control Syst Technol. 1998;6(3):412–420.
[18] Orosz G, Krauskopf B, Wilson RE. Bifurcations and multiple traffic jams in a vehicle-following model with reaction-time delay. Physica D. 2005;21:277–293.
[19] Pacejka H. Nonlinearities in road vehicle dynamics. Vehicle Syst Dyn. 1986;15(5):237–254.
[20] Palkovics L, Venhovens PJT. Investigation on stability and possible chaotic motions in the controlled wheel suspension system. Vehicle Syst Dyn. 1992;21:269–296.
[21] Shavrin PA. A chaotic dynamics of the vehicle on the plane. Proceedings of the international conference on physics and control; 2005; St. Petersburg. p. 474–478.
[22] Zhu Q, Ishitobi M. Chaos and bifurcations in a non linear vehicle model. J Sound Vib. 2004;275:1136–1146.
[23] Pacejka H. Tire and vehicle dynamics. 2nd ed. Elsevier; 2006.
[24] Pacejka H. Simplified analysis of steady-state turning. Vehicle Syst Dyn. 1973;21:269–296.
[25] Dhooge A, Govaerts W, Kuznetsov YuA. MATCONT: A MATLAB package for numerical bifurcation analysis of ODEs. ACM Trans Math Software. 2003;29(2):141–164.
[26] Doedel EJ, Champneys AR, Fairgrieve T, Kuznetsov YuA, Oldeman B, Paffenroth R, Sandstede B, Wang X, Zhang C. AUTO-07P : continuation and bifurcation software for ordinary differential equations, 2007. Available from: www.dam.brown.edu/people/sandsted/auto/auto07p.pdf
[27] True H. Multiple attractors and critical parameters and how to find them numerically: the right, the wrong and the gambling way. Vehicle Syst Dyn. 2013;51(3):443–459.